Plasma analysis for the plasma immersion ion implantation processing by a PIC-MCC simulation

Y. Miyagawa [a,*], M. Ikeyama [a], S. Miyagawa [a], M. Tanaka [b], H. Nakadate [b]

[a] *National Institute of Advanced Industrial Science and Technology (AIST Chubu), Shimo-shidami, Moriyama-ku, Nagoya, 463-8560 Japan*

[b] *PEGASUS Software Inc., Hatcho-bori, Chuo-ku, Tokyo, 104-0032 Japan URL http://www.psinc.co.jp/*

Abstract

In order to analyze the plasma behavior during PIII processing, a computer simulation has been carried out using the simulation software "PEGASUS". The software uses a particle in cell (PIC) method for the movement of charged particles in the electromagnetic field and a Monte Carlo method for collisions of ions, electrons, and neutrals in the plasma and also a Monte Carlo method to analyze the background gas behavior for a low density gas system. This approach is based on the weighting collision simulation scheme allowing for disparate number densities of different species. The spatial distributions of potential and densities of ions, electrons and radicals in the coating system were calculated together with the flux of ions and electrons on the surface of the object. The gas pressure was 0.01 to 50 Pa and a negative and/or a positive pulse voltage (V_{max} = 0.1 to 20 kV) was applied to the object. The calculation is fully self-consistent. A two-dimensional Cartesian and a cylindrical coordinate system were used. The effects of gas pressure, applied voltage, and secondary electron emission coefficient by ion impact (γ) on the sheath thickness, the spatial distribution of densities of electron, ion, and neutral atoms, the ion flux and its spatial distribution, etc. were studied for PIII processing of a trench shaped object, inner wall of a pipe and a PET bottle.

Key words: PIC-MCC simulation, PIII, Plasma Immersed Ion Implantation, PIC-MCC coupling simulation

1. Introduction

Plasma Immersion Ion Implantation (PIII) was originally conceived as a method for high-flux implantation and conformal implantation on a complex shaped object [1]. In PIII, a negative pulsed high voltage is applied to the object immersed in low-pressure high-density plasma. Then, ion sheath is formed around the object and energetic ions are implanted on the object surface. The higher the plasma density is, the thinner the sheath is, so, conformal implantation is possible in high-density plasma. However, it can't be easily realized for a complex shaped object, for instance, which has a trench or holes with high aspect ratio. In order to analyze the plasma and to find the most appropriate condition for the process, computer simulation is quite useful. For this purpose, simulations based on several models have been performed [2,3]. We have used the simulation software "PEGASUS" [4]. The software uses the PIC-MCC method together with the dynamic-SASAMAL code [9,10] for the ion-solid surface interactions. PEGASUS is consisted of many modules and the user can choose a proper set of modules which fit to the purpose considering the calculation time and the preciseness.

* Corresponding author.
Email address: y.miyagawa@arion.ocn.ne.jp (Y. Miyagawa).

2. Simulation Method

The outline of the PEGASUS using PIC-MCC module is given in Ref. [4]. Depending on the gas density and the calculation time, PEGASUS uses each two modules: for plasma simulation, Plasma Hybrid Module (PHM) and the Particle-in-Cell-Monte Carlo Collision Module (PIC-MCCM) and for the simulation of gas field, the Neutral Momentum Equation Module (NMEM) and the Direct Simulation Monte Carlo Module (DSMCM). PIC-MCCM and DSMCM are used for a low-density gas system, which is used in PIII. The Neumann boundary condition is applied to the open boundary. In general, the calculation time is from several to several ten hours with a windows machine of Pentium 4-2 GHz. In a real condition, when the discharge starts and the target-current intensity increases, the applied voltage decreases to some level following the power limit of the system. And then, the target current is kept on a limited level. However, such effect is not included in PEGASUS, so far. So that, when a discharge starts, the plasma density increases without a limit.

3. Results and Discussions

3.1. *Sheath expansion around a trench shaped object[4,7]*

In PIII, a negative pulsed high voltage is applied to the object immersed in a low-pressure high-density plasma. The simulations were performed for such PIII condition with a trench shaped object. The object shape, which is immersed in Ar plasma (0.133 Pa, 10^{16} m^{-3}) and the pulse shape of the applied voltage are shown in Fig. 1 together with the time evolution of the spatial distribution of electron density around the object. It is clearly shown that conformality is realized only at the beginning of the pulse when the voltage is rising. The time dependence of sheath length and ion flux at the flat part P_1 for maximum voltages of 2, 5 and 20 kV were obtained and compared with the analytical results based on the Child-Langmuir theory [5]. The agreements are satisfactory for all voltages. The ion fluxes along the object surface obtained by the similar simulation are shown in Fig. 2. The x-axis shows the distance from the center of the bottom surface of the trench. The ion flux on the inside wall is low, especially after 1 μs when the voltage

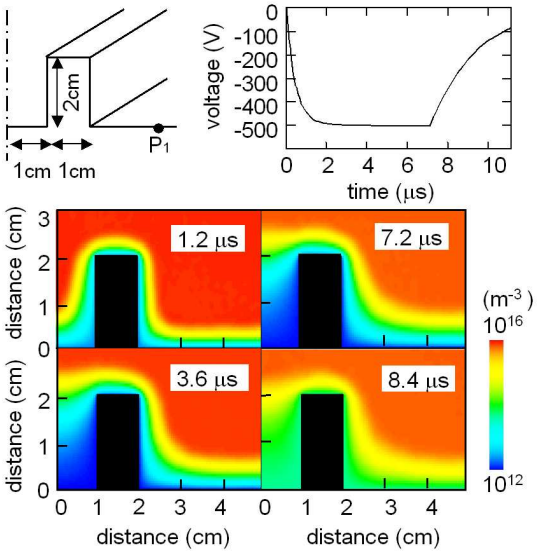

Fig. 1. Time evolution of Ar plasma with a negative pulsed voltage applied to the target. The upper, left figure shows the size of the object. The upper right is the applied voltage to the object. V_{max} = -500V. Ar gas pressure = 0.133Pa. γ=1. Initial plasma density = $10^{16}m^{-3}$.

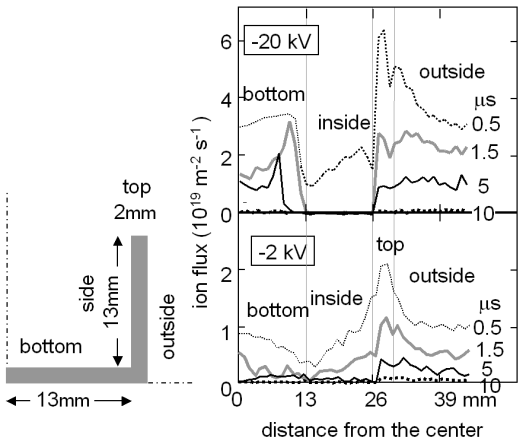

Fig. 2. Ion flux along the object surface at different times. The object shape is also shown. Ar gas pressure =0.133 Pa. Initial plasma density = $10^{16}m^{-3}$.

reaches the maximum value, because of the sheath expansion. The ion flux on the top and outside of the trench quickly decreases with time at first, until the voltage reaches a maximum (1.5 μs), and then decreases slowly. The depression of ion flux on the inside surface of the trench shaped object agreed with Keller's results [3].

3.2. *Hollow cathode discharge plasma for inner coating of a pipe[7,9]*

There is great commercial interest in coating on the inside surfaces of pipes and holes. When a negative voltage is applied to a cylindrical object, a high-density plasma is generated inside of the object as a result of hollow cathode discharge effect under a special condition. Figure 3 shows the results for a pipe (r = 2cm, l = 5cm) in 50 Pa Ar. When a negative voltage is applied to the object, electrons move off the object quickly, and as a result, plasma is generated by electron collisions with gas atoms between the pipe edge and the anode. Then, the plasma goes into the pipe. Finally, at 1.2 μs, pendulum motion starts and hollow cathode plasma (HCP) develops [10]. The electron flux shows that such motion takes place at this moment. Simulations were performed with various values for the gas pressure, the radius, the length, V_{max}, and γ. Secondary electron emission from the cathode surface (γ) plays an important role in HCP together with the gas pressure. With low γ, HCP is not generated. In a too low-pressure gas, HCP is neither generated. The plasma generation inside of cm-sized and mm-sized pipe in Ar gas with γ =1 is summarized in Fig. 4. The thick solid line and the thick broken line were obtained as a Paschen-like curve for HCP inside of cm-sized and mm-sized pipe, respectively. The HCP condition for the mm-sized pipe is much severe than cm-sized pipe although the area where HCP is generated is in the middle of the area for a cm-sized pipe. A similar Paschen-like curve for a HCP in He gas was obtained by Eichhorn et al. by an analytical method [11]. Their Paschen curve also shifted towards lower pressure than that of ordinary Paschen curve.

All above results are for a pipe of aspect ratio (l/r) of 5 or 2.5. It was found that a hollow cathode plasma works well for a short pipe (1/r < 7). But, for a long pipe with high aspect ratio, plasma intensity at the middle part was not satisfactory. Simulations were performed for a pipe with a grounded rod on the center. Intense plasma is generated in such system and it works how long the pipe is. Experiments have been performed using the condition obtained by the simulation and inner DLC coating of pipes of high aspect ratio was realized.

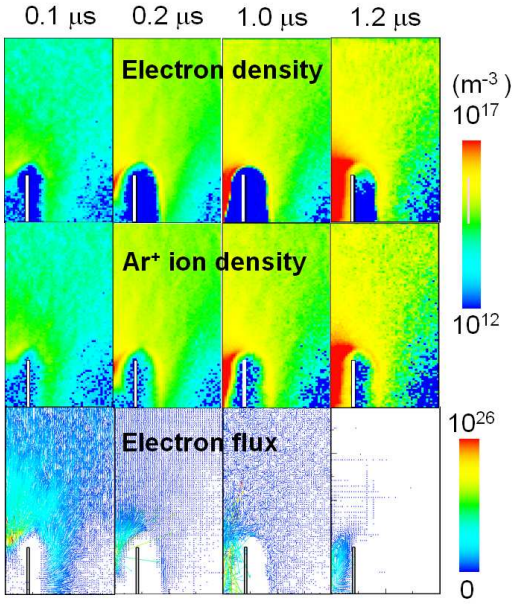

Fig. 3. Time evolutions of electron density, Ar ion density, and electron flux. 50 Pa Ar. V_{max} = -1kV. γ = 1. A cylindrical coordinate system was used.

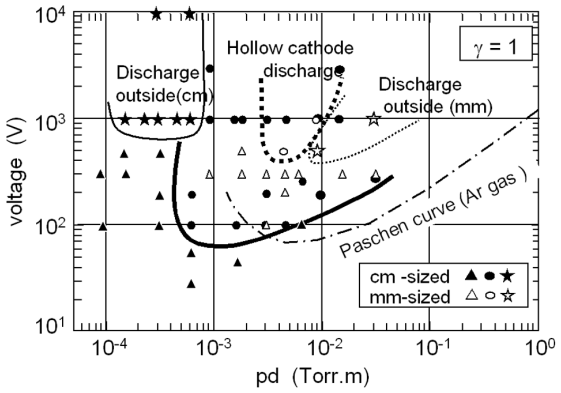

Fig. 4. Summary of hollow cathode plasma generation for a cm-sized and a mm-sized pipe. Pd vs. voltage, where p is pressure and d is radius. The ordinary Paschen curve is also shown. γ = 1. ● ○ Hollow cathode plasma discharge is generated. ★ ☆ Discharge starts outside of the pipe under low pressure and high voltage. ▲ △ Plasma is not generated.

3.3. *Inner coating of a PET bottle[12,13]*

In recent years, the inner coating of a PET (polyethylene terephthalate) bottle with DLC has gathered much interest because it drastically decreases the permeability of oxygen and other gases. At first, the gas flow field is simulated by DSMCM until it reaches the steady state. Then, coupling

simulation of the DSMCM and PIC-MCCM is performed. The pressure distribution obtained by DSMCM after it reaches the steady state is shown in Fig. 5 for N_2 gas. The inlet graph shows the pressure distribution at the height of 50 mm (along the dot-broken line). Time evolutions of spatial distribution of densities of electron, N_2^+ ion, N atom and N_2^* radical were obtained. The plasma density increases even after the applied voltage was cut off at 5 μs. It resulted from the electron movement just after the voltage was cut off. However, the flux of energetic ions on the inside surface of the bottle decreased quickly after the voltage was off.

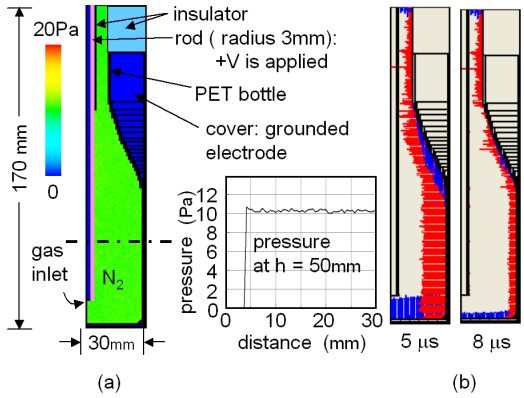

Fig. 5. (a) N_2 gas pressure distribution obtained by DSMCM after it reaches the steady state. (b) Energy flux of N_2^+ ion on the inner surface at 5 μs (V=-500V) and at 8 μs (V=0). The inlet graph shows the pressure distribution at the height of 50 mm (along the dot-broken line). 5 sccm. V_{max} = 500V. γ = 1.

Simulations were also performed with various values of γ and the pressure. In all cases plasma density increases after the voltage was off, and then slowly decreases. It was observed experimentally that the Ar plasma density decreased to the half level after 600 μs from the voltage cut off [14]. Although the simulation was for N_2 plasma at 10 Pa with V_{max} of 500V and the experiment is for Ar plasma with V_{max} of 1 kV, both values agreed well. The agreement resulted from the similarity in the collision cross sections for both systems. In the case of 10 Pa with the pulse length of 5 μs and γ = 0.5, at 6 to 10 μs, N_2^+ ion density is 4×10^{15} m^{-3} and N_2^* radical density is 4×10^{16} m^{-3}, so the N_2^+ ion / N_2^* radical ratio was about 0.1. The ion to radical ratio decreased with the increase of gas pressure. The N^+ ion density was negligible for all cases.

4. Summary

In order to analyze the plasma behavior in the PIII process, some simulation were carried out using the simulation software "PEGASUS". For plasma behavior in the surroundings of a trench shaped object immersed in high density Ar plasma, the time dependence of sheath length and ion flux on the flat part of the surface agreed with the analytical values obtained by the Child-Langmuir method. For inside coating of a pipe, Paschen-like curve for a hollow cathode discharge were obtained for both cm-sized and mm-sized pipe. By inserting a grounded rod on the center of pipe, a high-density glow discharge plasma is generated which spread whole inside of the pipe regardless of the length. It works very well for inner coating of a pipe of high aspect ratio. Ar and N_2 plasma inside of a PET bottle with a thin gas inlet on the center of the bottle was also simulated for DLC coating to the inner surface of a bottle and it was confirmed it works very well.

References

[1] A. Anders, Mater. Chem. Phys. 17 (1987) 485; Handbook of Plasma Immersion Ion Implantation and Deposition, John Wiley and Sons, New York, 2000.

[2] R. A. Stewart and M. A. Lieberman, J. Appl. Phys. 70 (1991) 3481.

[3] G. Keller, U. Rude, L. Stals, S. Mandel, and B. Rauschenbach, J. Appl. Physics 88 (2000) 1111.

[4] Y. Miyagawa, M. Ikeyama, S. Miyagawa, H. Nakadate, Nucl. Instr. and Meth. B206 (2003) 767.

[5] Y. Miyagawa, M. Ikeyama, K. Saito, G. Massouras and S. Miyagawa, J. Appl. Phys. 70 (1991) 7289.

[6] Y. Miyagawa, H. Nakadate, M. Tanaka and S. Miyagawa, Surf. & Coat. Tech. 156 (2002) 87.

[7] Y. Miyagawa, H. Nakadate, M. Tanaka, M. Ikeyama, S. Miyagawa, Surf. & Coat. Tech. 186 (2004) 2.

[8] J. R. Conrad, J. Appl. Phys. 62 (1987) 777.

[9] Y. Miyagawa, H. Nakadate, M. Tanaka, M. Ikeyama, S. Miyagawa, Surf. & Coat. Tech. 196 (2005) 155.

[10] H. Pak and M. J. Kushner, J. Appl. Phys. 71 (1992) 94.

[11] H. Eichhorn, K. H. Schoenbach, T. Tessnow, Appl. Phys. Lett. 63 (1993) 2481.

[12] Y. Miyagawa, H. Nakadate, M. Tanaka, M. Ikeyama, S. Miyagawa, Nucl. Instr. & Meth. B242 (2006) 341.

[13] Y. Miyagawa, M. Tanaka, H. Nakadate, M. Ikeyama, S. Miyagawa, Plasma Process. Polim. 2 (2005) 480.